Available online at www.sciencedirect.com

ScienceDirect

Procedia CIRP 118 (2023) 890–894

www.elsevier.com/locate/procedia

16th CIRP Conference on Intelligent Computation in Manufacturing Engineering, CIRP ICME '22, Italy

Laser welding of AA2065 and AA7021Al Alloys using purpose made welding wires

Siri Marthe Arbo[a], Kristian Martinsen[a,*], Jo Aunemo[a], Nora Dahle

[a] *SINTEF Manufacturing AS, PO Box 163, 2831 Raufoss, Norway*

* Corresponding author. Tel.: +47 99521849; *E-mail address:* Kristian.martinsen@sintef.no

Abstract

Aerospace AA2xxx and AA7xxx alloys have good mechanical properties such as high strength-to-weight ratio, fatigue- and corrosion resistance. These alloys are known for poor weldability with traditional fusion welding techniques due to hot cracking sensitivity and large heat affected zone with reduced mechanical properties. This paper describes laser welding of AA2065 and AA7021 alloys applying a purpose made wire for added weld material. The welding was made in a laser metal deposition machine with wire feeding and Argon shield gas. The work demonstrates promising results for joining of these alloys with added material, showing weld strength similar to base material. Porosity is, however, still a challenge that must be controlled by optimizing the welding process.

Keywords: Laser welding; Aluminium alloy; Wire laser letal deposition

1. Introduction

Aerospace grade AA2xxx and AA7xxx Aluminium (Al) alloys are known for good mechanical properties such as high strength-to-weight ratio as well as high fatigue- and corrosion resistance. These alloys are interesting to use in structural components where weight saving is crucial, such as aviation and space industry [1-3]. The alloys are, however, known to be challenging to weld with poor weldability using traditional fusion welding techniques due to hot cracking sensitivity and the formation of heat-affected zones adjacent to the weld with reduced mechanical properties [4-10].

A method that has proven suited for welding of Al alloys is laser beam welding. The small beam size and accuracy provides control of the microstructure, a relatively small heat-affected zone (HAZ), rapid solidification and less recrystallization and grain growth [1, 9]. Laser welding these metals still suffers, however, from "*weld seam irregularities such as notches or holes, which reduce the mechanical properties of the join" [6].* Similar challenges are reported by Campbell [4], Madhusudhan [7], Xiao and Zhang [8] as well as Çam and İpekoğlu [9]. Çam and İpekoğlu reviewed Al alloys laser welding, focusing on porosity, cracking, resulting microstructure and mechanical properties.

Previous work [10] have demonstrated that that also 2xxx Al-Cu-Li and 7xxx Al-Zn-Mg alloys can be laser welded. Neither of these authors have however, used wires as filler in the weld seams. For certain weld geometries filler material is necessary such as larger gaps, thicker materials etc. Furthermore has filler material proven to create high quality, robust welds in other applications of laser welding: As stated in [15]: "*Laser welding using filler wire has been proven effective in producing high quality, robust welds with improved fit-up, reduced weld cracking and better weld profile*."

The focus of the study presented in this paper was to investigate if wires made from AA2065 Al-Cu-Li and AA7021 Al-Zn-Mg alloys could be utilized for laser welding of these alloys. The hypothesis was that by using wires with equal chemical composition as the base materials, the whole joint structure could be heat treated to ensure equal strength in the weld and substrate material. Hence, the strength of the weld would not be the critical design feature. There is, however, no commercially available wires for these materials, and the authors decided to produce a purpose made weld wire by themselves for these experiments.

2. Method and experimental setup

2.1. Materials

The plates and the wires were produced from the same casted AA2065 and AA7021 billets. The chemical composition for the two alloys is presented in Table 1. The wires, with diameter of 1.2 mm were produced through extrusion and wiredrawing,

10.1016/j.procir.2023.06.153

combined with subsequent annealing at 410°C for 2 hours. The wires were used in as-fabricated conditions, containing some small surface wounds, and a homogeneous microstructure and particle distribution. The base material, 2 mm thick plates were produced through extrusion and cut into specimens for welding, 30x50 mm. The AA2065 and AA7021 plates were used in T4 condition during welding, by heat treatment at 530°C and 480°C for 30 minutes, respectively, one week prior.

Table 1 Chemical composition of AA2065 and AA7021 [wt%]

Alloy	Li	Cu	Zn	Mg	Mn	Zr	Ag	Fe	Si
AA2065	1.0	4.4	-	0.3	0.4	0.1	0.2	0.05	0.02
AA7021	-	0.3	5.9	1.7	-	0.1	-	0.09	0.04

2.2. Laser Metal Deposition setup

A single v-groove butt-joint was produced and the welding was performed using a Trumpf TruLaser Cell 3000 5-axis axis laser wire metal deposition machine. The experimental setup is illustrated in Fig. 1. The plates were machined prior to welding to give a bead angle of 60° and welding root of 0.3 mm. The weld was produced perpendicular to the extrusion direction of the plates. The laser was generated with a 400 µm fiber, rectangular pulse with a frequency of 5010 Hz. The spot size was 890 µm and 880 µm for AA2065 and AA7021 trials, respectively. The following process parameters were used for both alloys; Wire-feed rate (V_f): 1.9 m/min, Laser Power (P): 2700W, 2750W and 2800W, Welding speed (V_s): 1 m/min. Argon gas was used as shielding gas with a gas rate of 15 L/min.

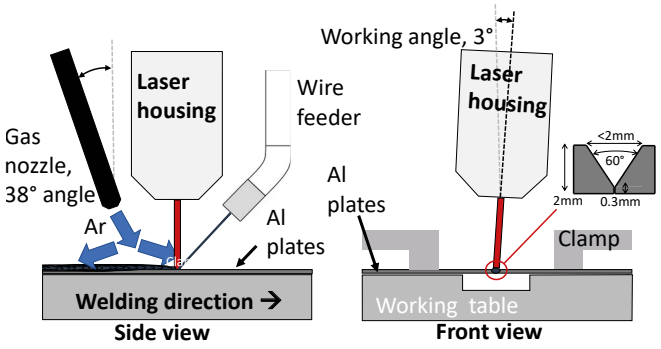

Figure 1. Illustration of the experimental setup

2.3. Post-welding heat treatments and characterization

The specimens were heat treated after welding, to T6 condition following two procedures. The first included only aging after welding (referred to as Aged AW). The second included solution heat treatment followed by aging (referred to as T6).
For AA2065, solution heat treatment was performed at 530°C for 30 min and aging was performed at 175°C for 24 hours. For AA7021, solution heat treatment was performed at 480°C for 30 min. Aging was performed at 100°C for 5 hours + 150°C for 6 hours. The heat-treated specimens were compared to the as-welded specimens to evaluate the effect of the post-welding heat treatments on mechanical properties. Cross-sections of the produced welds were ground and polished according to standard metallographic procedures. The porosity, particle structure and weld characteristics were evaluated using Zeiss Axio Observed optical microscopy and Hitachi S-3500N Scanning Electron Microscopy (SEM), operated at 20 kV and working distance: 15 and 25 mm. To evaluate the micro-structure, the polished specimens were anodized using Barkers Reagent (5% HBF4 in water, 20 V for 60 sec) followed by analyses using polarized light.
Vickers hardness measurements were obtained using a Tukon 2500 machine (HV0.5). A 500 µm distance was kept between each indent. Tensile testing was performed on specimens extracted perpendicular to the weld and from the substrate materials with dimensions according to ASTM E8. After testing, the fracture surfaces were examined in the SEM using the operating parameters presented previously.

3. Results

3.1. Mechanical properties

The results from the tensile tests for AA7021 and AA2065 are presented in Fig. 2 (a) and (b), respectively. The tensile strength is presented for as-welded, aged AW and T6 conditions. The laser power used to produce the welds are also presented. It is only for the welds subjected to T6 post-welding heat treatment that a laser power of 2750W and 2800W was used. Information on yield strength, elongation, hardness in the weld, joint efficiency (% of substrate material strength) and fracture location is listed in Table 2 for the joints produced with laser power of 2700W.
For AA7021, a clear increase in tensile strength was found when performing post-welding heat treatments, see Fig. 2 (a). After the T6 post-welding heat treatment, the strength of the weld reach 95-99% of the substrate material strength, and the fracture occurred either in the substrate adjacent to the weld or in the weld. The Aged AW heat treatment did increase the strength compared to the as-welded condition, and a joint efficiency of only 63% was reached. As seen from Table 2, the aged AW specimens also had poor ductility, and no elongation measured during tensile testing. For the T6 specimens, the elongation was similar to the substrate material at around 13-14% at fracture. For the AA7021 specimens, no difference could be observed between the welds produced with different laser powers, the same tensile strength was achieved.
For the AA2065 weld, the strength of the welds did not reach the strength of the substrate material, and for all tests, the fracture occurred in the weld, see Table 2. Overall, the achieved strength increased when performing post-welding T6 heat treatment, while no improvement was observed for the aged AW heat treatment, see Fig. 2 (b). The T6 specimens reached a joint efficiency of 84% in the welds produced with laser power of 2700W. For the T6 welds produced with laser power of 2750W and 2800W, a joint efficiency of 70% was achieved. However, as can be seen for all tensile tests in Table 2, hardly any elongation was measured during the tests. This result in an elongation of 0% for the AA2065 specimens.
The conducted hardness measurements confirm that the weld, after the T6 heat treatment reached a similar hardness as the substrate material, a T6 state. For the aged AW welds, the hardness increased compared to the as-welded condition.

Table 2. Main results from tensile testes for AA7021 and AA2065.

Alloy	State	Yield strength [MPa]	Tensile strength [MPa]	Elongation [%]	Joint efficiency [%]	Hardness in weld [HV0.5]	Fracture location
AA7021	Base Mat.	436	456	15	-	154-156	
AA7021	As welded	136	236	9.2	52	74-86	Weld
AA7021	Aged AW	-	287	0	63	95-105	Weld
AA7021	T6, P=2700W	437	434-453	13	95-99	136-146	Weld and substrate material
AA2065	Base Mat.	582	636	6	-	190-193	
AA2065	As welded	0	150	0	24	81-89	Weld
AA2065	Aged AW	0	34	0	5	97-103	Weld
AA2065	T6, P=2700W	0	467-531	0	74-84	165-188	Weld

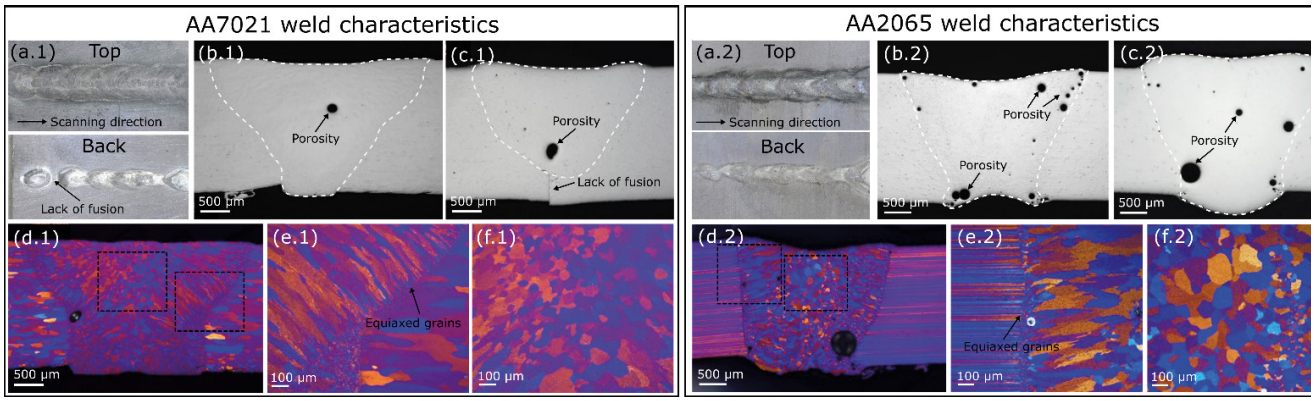

Fig. 3. Overview of the characteristics of the AA7021 and AA2065 welds. (a.X) shows images of typical weld appearance produced with P=2700W. (b.X) and (c.X) shows polished cross-sections. (d.X)-(f.X) shows the microstructure in the weld with high magnification images along the fusion line and in the centre of the weld.

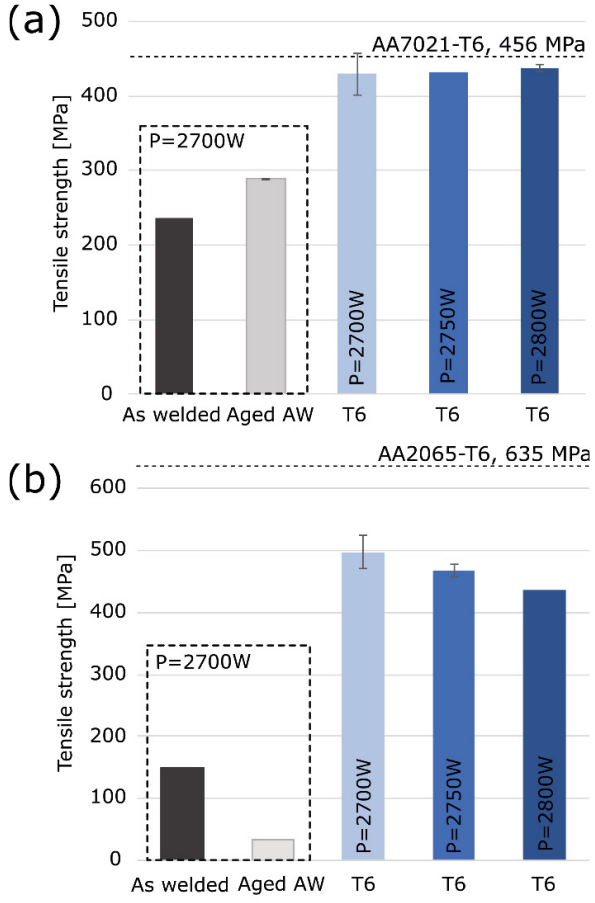

Fig. 2. Tensile strength of the (a) AA7021 welds and (b) AA2065 welds in as-welded, aged AW and T6 condition.

3.2. Weld appearance and microstructure

An overview of the typical weld appearance observed defects and microstructure is presented in Fig. 3. In general, the welds had a consistent appearance, although some areas indicate lack of fusion between the plates due to incomplete penetration, as indicated for AA7021 in Fig. 3 (a.1). Few or no defects could be observed on the surface. Lack of fusion could again be observed during the analysis of the cross-section, as shown in Fig. 3 (c.1). Some porosity was observed in the AA7021 specimens, although it is generally low and no influence on porosity could be observed when increasing the laser power to 2750W and 2800W. In comparison with AA7021, higher porosity was observed on the cross-sections of the AA2065 welds, as seen in Fig. 3 (b.2) and (c.2). All the observed pores are spherical and located at random positions throughout the welded material. The microstructure in the welds produced both with AA7021 and AA2065 could be divided into two categories. Along the fusion boundary, elongated grains growing perpendicular to the fusion boundary are observed. Small fine equiaxed grains were also observed at the fusion boundary, see Fig. 3 (e.1) and (e.2). In the centre of the welds, the microstructure consisted of equiaxed grains, Fig. 3 (f.1) and (f.2). The microstructure was not observed to change after the post-welding heat treatments for the two alloys and not with increasing laser power.

3.3. Fracture surfaces

The tensile test specimen fracture surfaces were examined further in the SEM to determine the fracture mechanism, focusing on the T6 welds. The fracture morphology for representable specimens for AA7021 and AA2065 are presented in Fig. 4.

For the AA7021 welds in T6 condition, the fracture either occurred in the substrate material or in the weld, with a joint efficiency at 95-99%. For the specimens shown in Fig. 4 (a)-(c), at the bottom of the weld, the previously defined defects are again observed, i.e., an area with lack of fusion and one large pore. The rest of the fracture surface indicates a ductile fracture, as dimples can be observed in the top region of the weld, see Fig. 4 (c).

The fracture surfaces from the AA2065 welds clearly shows the distribution of pores in the welds, see Fig. 4 (d) and (e). For this specimen, most of the porosity was located towards the bottom of the weld. The upper part of the weld shows signs of intergranular fracture with large flat surfaces, see Fig 4 (f).

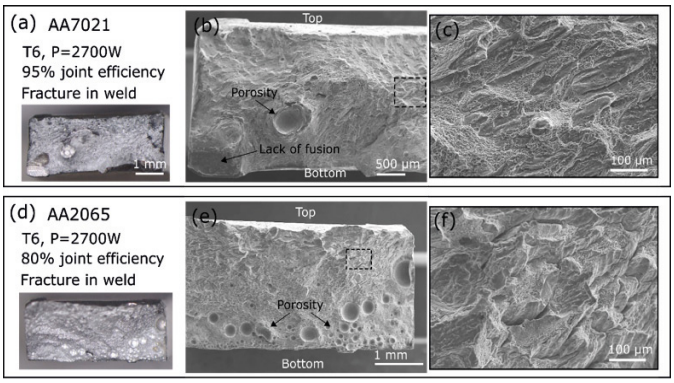

Fig. 4. racture surface characteristics for the T6 post-welding heat treated specimens for welds produced with laser power of 2700 W. (a) AA7021 fracture surface. (b) AA2065 fracture surface.

4. Discussion

The presented work demonstrates that self-produced wires made from AA7021 and AA2065 may well be used for laser welding of these alloys. Post-welding heat treatment was found to be necessary to achieve a high strength weld. The results show that welding with filler wire with similar chemical composition as the substrate material allows for making welded structures in AA7021 where the weld is as strong as the base material. For AA2065 further, investigations are required to find methods of pore elimination to obtain high quality welding of this material.

The quality and properties of the final weld are, however strongly affected by defect formation such as pores and lack of fusion, and post-welding heat treatments are necessary to reach the wanted strengths. Lack of fusion in the weld root was observed in some of the AA7021 welds, and a possible reason can be that during welding the wire was in some cases curved, as well as uneven feeding of the wire. This resulted in some lack of filler material at certain places, uneven melting of the wire and an instability in the production of the weld. To avoid this in future experiments, the wire must be processed further to minimize any curvature and allowing more stable wire feeding.

Porosity effects was found to be a neglectable for the AA7021 alloy with the current weld geometry and process parameters. Other studies have demonstrated similar positive results for Al-Zn-Mg alloys during laser welding [10]. Porosity was found to be a larger challenge for the AA2065 welds, on the other hand. Porosity is reported by other authors in Al-Cu-Li alloys welds as well [12, 13], and it has been argued that the alloy is especially prone to porosity formation as Mg and Li evaporates easily during the welding process. The evaporation promotes formation of pores, as well as hydrogen porosity [12, 13].

In previous work by the authors [16], the same A2065 wire was used for wire LMD on top of an AA7475 substrate plate. In these experiments, very few pores were formed. The authors mean there is a potential in optimising the process parameters and a quality in-control welding of these alloys should be possible, but further work is needed to accomplish this (especially for AA2065) when performing groove welding with wires.

The microstructure observed in the welds is typical for laser welded aluminium structures, with equiaxed grains in the centre of the weld as a result of the high cooling rates associated with this welding technique and elongated grains adjacent to the fusion boundaries [10, 12-15].

Both AA2065 and AA7021 are heat treatable alloys, meaning that their strength is dependent on the heat treatment the alloys are subjected to. The results show that only performing an aging heat treatment after welding is not sufficient to achieve a T6 condition in the weld material. Thus, a low hardness and strength were obtained in these welds even with the high cooling rate during solidification, see Table 2. However, the measured hardness and achieved mechanical properties show that a T6 condition was achieved in the weld material after the post-welding T6 heat treatment. For the AA7021 welds, the strength of the weld material reached that substrate material strength (90-99%). The fracture did however occur in the weld due to the presence of defects in some cases. For AA2065, the large amount of porosity negatively influenced the mechanical properties, only reaching 75-85% of the substrate material strength. However, by eliminating the porosity, the weld material has the potential of reaching strength equal to the substrate material.

5. Conclusions

The presented work demonstrates that self-produced wires made from AA7021 and AA2065 may well be used for laser welding of these alloys, and the work can open up for new applications for welding of high-strength aluminium alloys. Post-welding heat treatment was found to be necessary to achieve a high strength weld. Overall, the results show that welding with a filler wire with similar chemical composition as the substrate material allows for producing welded structures of AA7021 where the weld is as strong as the substrate material. However, for the AA2065, further investigations are required to find methods for pore elimination to obtain high quality welds with this alloy. The following can be summarized: For AA2065 welds, a tensile strength of 450-500 MPa after post-welding T6 heat treatments (joint efficiency of 75-85%) was achieved. The welds were hampered with porosity, which was the main reason for fracture and lower tensile strength than the substrate material.

As for AA2065, the quality of the AA7021 welds were strongly influenced by post-welding heat treatment. The T6 heat treatment provided excellent mechanical properties with a tensile strength of 430-450 MPa (joint efficiency of 90-99%), with fracture occurring either in weld or substrate material. The fracture surfaces showed mainly ductile fractures. The study showed only small amounts of porosity and areas with lack of fusion in the AA7021 weld material. This reduced the weld material elongation to 10-13% compared to 15% in the substrate material.

Future work should focus on improving the wire, to ensure sta-

ble welding process, sufficient shield gas and eliminate potential defects such as lack of fusion. Finding new applications for these self-made wires should be further studied, for instance within additive manufacturing with laser-based techniques. The potential has already been demonstrated for wire-arc welding by Zhong et al. [17] for a self-produced wire AA2050 Al-Cu-Li.

1. Acknowledgements

The authors acknowledge the contribution from KA Rasmussen on producing the wires and SINTEF AS for funding the work.

References

[1] Rioja RJ, Liu J (2012) The Evolution of Al-Li Base Products for Aerospace and Space Applications. Metall Mater Trans A 43(9), pp3325-3337. https://doi.org/10.1007/s11661-012-1155-z
[2] Ahmed B, Wu SJ (2014) Aluminum Lithium Alloys (Al-Li-Cu-X)-New Generation Material for Aerospace Applications. Appl Mech Mater 440, pp104-111. https://doi.org/10.4028/www.scientific.net/AMM.440.104
[3] Dursun T, Soutis C (2014) Recent developments in advanced aircraft aluminium alloys. Mater Design 56, pp862-871. https://doi.org/10.1016/j.matdes.2013.12.002
[4] Campbell Jr FC (2011) Chapter 2 – Aluminum. In: Campbell Jr FC (ed) Manufacturing technology for aerospace structural materials. Elsevier Science, pp15-92.
[5] Martinsen et al. (2015) Joining of dissimilar materials, CIRP Annals – vol 64-2, pp679–699. https://doi.org/10.1016/j.cirp.2015.05.006
[6] Schmidt et al (2018) Advances in macro-scale laser processing, CIRP Annals 67(2), pp719-742. https://doi.org/10.1016/j.cirp.2018.05.006
[7] Madhusudhan Reddy G, Gokhale AA (2014) Chapter 9 - Welding Aspects of Aluminum–Lithium Alloys. In: Prasad NE, Gokhale AA, Wanhill RJH (ed) Aluminum-lithium Alloys: Processing, Properties, and Applications, Butterworth-Heinemann Elsevier, Boston, pp 259-302.
[8] Xiao R, Zhang X (2014) Problems and issues in laser beam welding of aluminum–lithium alloys. J Manuf Process 16(2), pp166-175. https://doi.org/10.1016/j.jmapro.2013.10.005
[9] Çam G, İpekoğlu G (2016) Recent developments in joining of aluminum alloys. Int J Adv Manuf Technol 91(5-8), pp1851-1866. https://doi.org/10.1007/s00170-016-9861-0
[10] Zhang et al. (2015) Microstructure and mechanical properties of a new Al–Zn–Mg–Cu alloy joints welded by laser beam, Mater Design 83, pp451–458. https://doi.org/10.1016/j.matdes.2015.06.070
[11] Feng et al. (2014) Microstructure and mechanical properties of laser beam welded AA7021Aluminum alloy, Appl Mech Mater 488-489. pp 106-110. https://doi.org/10.4028/www.scientific.net/AMM.488-489.106
[12] Gu et al. (2017) Investigation of welding parameters on microstructure and mechanical properties of laser beam-welded joint of 2060 Al-Cu-Li alloy, Int J Adv Manuf Technol 91, pp771-780. https://doi.org/10.1007/s00170-016-9806-7
[13] Liu et al. (2018) Microstructure and mechanical properties of laser welded joints between 2198/2060 Al-Li alloys, Mater Sci Technol 34(1), pp111-122. https://doi.org/10.1080/02670836.2017.1365221
[14] Molian, PA, Srivatsan TS (1990) Weldability of aluminium-lithium alloy 2090 using laser welding, J Mater Sci 25, pp3347-3358
[15] Mohammed Naeem, 2020, High-Power Fiber Laser Welding With Filler Material, SME.org, https://www.sme.org/technologies/articles/2020/july/high-power-fiber-laser-welding-with-filler-material/
[16] Arbo et al. (2022) On weldability of aerospace grade Al-Cu-Li alloy AA2065 by wire-feed laser metal deposition, J Adv. Joining Process 5(100096) https://doi.org/10.1016/j.jajp.2022.100096
[17] Zhong et al. (2019) Microstructure and mechanical properties of wire+arc additively manufactured 2050 Al-Li alloy wall deposits, Chin J Mech Eng, 32(92). https://doi.org/10.1186/s10033-019-0405-z